OBSERVATIONS OF TeV GAMMA-RAY FLARES FROM MARKARIAN 501 WITH THE TELESCOPE ARRAY PROTOTYPE

N. HAYASHIDA,[1] H. HIRASAWA,[1] F. ISHIKAWA,[1] H. LAFOUX,[1] M. NAGANO,[1] D. NISHIKAWA,[1] T. OUCHI,[1] H. OHOKA,[1]
M. OHNISHI,[1] N. SAKAKI,[1] M. SASAKI,[1] H. SHIMODAIRA,[1] M. TESHIMA,[1] R. TORII,[1] T. YAMAMOTO,[1] S. YOSHIDA,[1]
T. YUDA,[1] Y. HAYASHI,[2] N. ITO,[2] S. KAWAKAMI,[2] Y. KAWASAKI,[2] T. MATSUYAMA,[2] M. SASANO,[2] T. TAKAHASHI,[2]
N. CHAMOTO,[3] F. KAJINO,[3] M. SAKATA,[3] T. SUGIYAMA,[3] M. TSUKIJI,[3] Y. YAMAMOTO,[3] N. INOUE,[4] E. KUSANO,[4]
K. MIZUTANI,[4] A. SHIOMI[4] K. HIBINO,[5] T. KASHIWAGI,[5] J. NISHIMURA[5] E. C. LOH,[6] P. SOKOLSKY,[6]
S. F. TAYLOR,[6] K. HONDA,[7] N. KAWASUMI,[7] I. TSUSHIMA,[7] Y. UCHIHORI,[8] H. KITAMURA,[9]
M. CHIKAWA,[10] S. KABE,[11] Y. MIZUMOTO,[12] H. YOSHII,[13] N. HOTTA,[14] To. SAITO,[15]
M. NISHIZAWA,[16] H. KURAMOCHI,[17] AND K. SAKUMOTO[17]

ABSTRACT

We report the observations of TeV gamma-ray flares from Markarian 501 using the Telescope Array Prototype. The observations were carried out continuously from the end of March to the end of July of 1997. The energy spectrum and the time variation of the gamma-ray intensities are shown. The intensity has been changed by an order of magnitude in this period, and the possible quasi-periodic oscillation of 12.7 days were discovered.

Subject headings: BL Lacertae objects: individual (Markarian 501) — gamma rays: observations

1. INTRODUCTION

Markarian 501 (Mrk 501) is an extragalactic BL Lacetae–type object at $z = 0.034$. It was observed in radio, optical, and X-ray bands and can be characterized as a flat-spectrum, radio, highly optically polarized, and optically violent variable. BL Lac type objects are considered to be a kind of active galactic nucleus (AGN) that have a jet oriented to our line of sight. Recently, Mrk 501 (Quinn et al. 1996; Bradbury et al. 1997), Mrk 421 (Punch et al. 1992; Petry et al. 1996; Aiso et al. 1997a), and 1ES 2344+514 (Catanese et al. 1997a) have been identified as TeV gamma-ray sources, and they are all BL Lac objects. Gamma rays from Mrk 501 around 100 MeV to 10 GeV were not observed by the *CGRO* EGRET detector (Shrader & Gehrels 1995); however, emission in the TeV energy region was discovered by the Whipple telescope (Quinn et al. 1996) and confirmed by the HEGRA telescopes (Bradbury et al. 1997). Detailed study of gamma rays from AGNs will give us information about the environment surrounding the huge black hole located at the center of the AGN and the high-energy phenomena and particle acceleration in the jet. The timescale of the intensity variations of the TeV gamma rays may explain why the particle acceleration site is close to the black holes. TeV gamma rays from such extragalactic objects interact with the infrared background photons, and a cutoff of the energy spectrum is expected around 7–15 TeV (Stecker & de Jager 1997). There is an ambiguity in the prediction of the cutoff energy resulting from the uncertainty of the number density of infrared photons. In the discovery stage, the intensity in the TeV energy range was very small, corresponding to 8% of the Crab Nebula flux; however, from 1997 March it increased dramatically and varied from 0.3 to 4 crab flux. It was found that the variation of the intensities were larger in the TeV range than in the X-ray and other ranges (Catanese et al. 1997b). These flares were observed by Whipple, HEGRA, CAT, TAC-TIC, and the Telescope Array Prototype (TAP) (Quinn et al. 1996; Bradbury et al. 1997; Barrau et al. 1997; C. L. Bhat 1997, private communication; Aiso et al. 1997b). The flares were continuously observed until the end of 1997 July. Here will report the details of the Mrk 501 observations by TAP.

2. EXPERIMENT

The Telescope Array Prototype detector (Aiso et al. 1997c), a seven-telescope array, is under construction at Dugway, Utah. Its geographical position is 40°33 N, 113°02 W, at an altitude of 1600 m above sea level. The prototype detector works in dual modes: the Cerenkov mode and the air fluorescence mode. Construction started in the summer of 1996, and currently three telescopes with the respective separation of 120 m are in operation. The seven telescopes will be arranged in a hexagonal grid with a separation of 70 m to maximize the detection efficiency of TeV gamma rays. Each telescope is alt-azimuth mounted with a 6 m² main dish. The main dish consists of 19 hexagonally shaped segmented mirrors coated with anodized aluminum. The reflectivity of the mirrors is about 90% at wavelength of 400 nm. At the focal plane, a high-resolution imaging camera of 256 channel photomultipliers is installed to measure detailed images of Cerenkov light from gamma rays and cosmic rays. The Cerenkov light images are used to distinguish the gamma rays from the huge number of background cosmic rays. The typical cosmic-ray rate is about 1000 minute⁻¹, and the gamma-ray rate from the Crab Nebula is about 0.5 minute⁻¹

[1] Institute for Cosmic Ray Research, University of Tokyo, Tokyo 188, Japan.
[2] Department of Physics, Osaka City University, Osaka 558, Japan.
[3] Department of Physics, Konan University, Kobe 658, Japan.
[4] Department of Physics, Saitama University, Urawa 338, Japan.
[5] Department of Engineering, Kanagawa University, Yokohama 221, Japan.
[6] Department of Physics, University of Utah.
[7] Faculty of Education, Yamanashi University, Kofu 400, Japan.
[8] The 3rd Research Group, National Institute of Radiological Sciences, Chiba 263, Japan.
[9] Department of Physics, Kobe University, Kobe 657, Japan.
[10] Department of Physics, Kinki University, Osaka 577, Japan.
[11] National Laboratory of High Energy Physics, Tsukuba 305, Japan.
[12] National Astronomical Observatory, Tokyo 181, Japan.
[13] Faculty of General Education, Ehime University, Ehime 790, Japan.
[14] Faculty of Education, Utsunomiya University, Utsunomiya 321, Japan.
[15] Tokyo Metropolitan Colleage of Aeronautical Engineering, Tokyo 116, Japan.
[16] National Center for Science Information System, Tokyo 112, Japan.
[17] Faculty of Science and Technology, Meisei University, Tokyo 191, Japan.
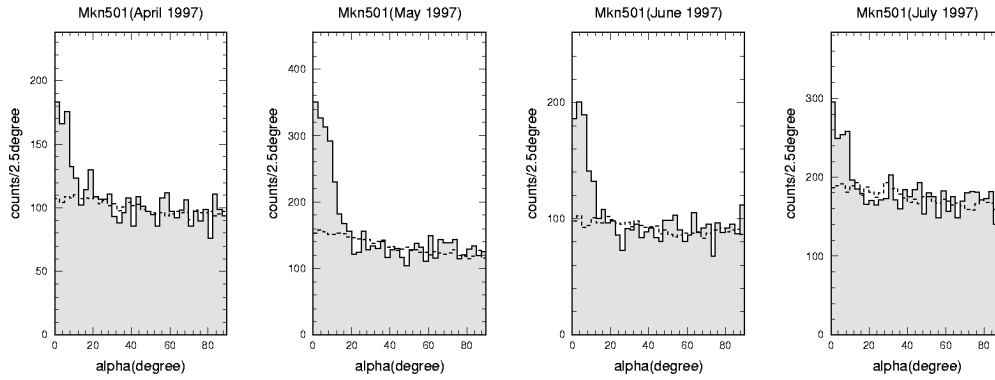
FIG. 1.—Monthly alpha distributions. Solid lines and broken lines show the alpha distribution for on-source and for off-source, respectively. The excess in the small alpha region ($\leq 15°$) corresponds to the gamma rays from Mrk 501. Total significance is more than 35 σ.

(Aiso et al. 1997b) with three telescopes. Therefore, rejection of cosmic-ray background events using the shape parameter of the Cerenkov light is essential to obtain a reasonable S/N ratio in this experiment, and we used the techniques originally developed by the Whipple group (Hillas 1985). The absolute pointing accuracy of the telescopes is typically $1'$, which is frequently calibrated by imaging bright stars.

The signals from the 256 channel camera were amplified just behind the camera in order to minimize electric noise and to obtain better timing resolution; they were then fed to ADC and TDC modules mounted at the telescope base to measure the amplitude and timing after passing through 10 m of twisted pair cables. The triggering requirement to record the event was four folds out of 256 tubes. The threshold of the discriminators were set at the five photoelectron level. The single counting rates in each tube were set to 3–5 kHz in each channel. The threshold energy for detectable gamma rays was 600 GeV for vertical showers. Mrk 501 was observed with the raster scan tracking mode. In this mode, the telescope tracking center scanned the square region of $\pm 0°5$ in right ascension and declination coordinate centered on the target. There are several advantages in this method compared with the conventional on-source/off-source tracking mode. The on-source and off-source sky region can be observed simultaneously. The systematics of the imaging devices can be reduced significantly. By observing the bright star images, the calibration of the telescope absolute direction can be done with the accuracy of $0°03$. Our telescopes will be described in more detail elsewhere.

This observation of Mrk 501 was carried out from the end of March to the end of 1997 July. We observed a total number of 47 nights for a total observation time of 105.4 hr. We observed 3,400,000 events in the field of view of $\pm 2°$ around Mrk 501, which are mainly cosmic-ray protons and helium nuclei. In the analysis, we limited the zenith angle to the range of 5°–25° in order to reduce the systematic errors in the energy and the aperture estimates. This left 2,160,000 events and 64.0 hr of live time, with an average event rate of 9.4 Hz with three telescopes. Among these events, we selected gamma-ray candidates using the shape parameters of Cerenkov images and their directionality. We can determine the arrival direction of gamma rays and the cosmic rays with an accuracy of $0°1 \times 0°3$ (the elliptical errors) in each event. Therefore, 97% of the background events around the target, say within $\pm 1°$, can be rejected. The cosmic rays showed larger images than gamma rays, and they were rejected with 95% efficiency through the image selection. Therefore, typically 99.85% [$\sim 1.0 - (1 -$

0.97)(1 − 0.95)] of the background events around the target were rejected with the image and the arrival direction using the present analysis method. 35% of the gamma rays remained through this process. Therefore, even if the original S/N is bad as 0.001, we can obtain S/N of order ~ 1.

3. ANALYSIS

At first, the clean Cerenkov images were obtained by removing the background photons with the timing information. The signal timings of each photomultiplier were recorded with an accuracy of 1 ns. The Cerenkov light signals from gamma rays and cosmic rays were concentrated within a 10 ns interval; however, noise—including the photons from star light and the air glow—was randomly distributed in time. Therefore, we required a timing alignment with a software gate set at 40 ns. After the timing selection, we required the clustering of hit tubes as follows. We defined clear hit tubes that are accompanied by two or more neighboring hit tubes. Then, the hit tubes were salvaged if the clear hit tube locates the neighborhood. We required four clear hit tubes and five hit tubes for event selection. After these selections and the image cleaning, the chance coincidence events caused by random coincidence were completely rejected and the pure Cerenkov events induced by gamma rays and cosmic rays remained.

Then the image parameters were calculated: signal size, *size*, the centroid position of images (x,y), *width*, *length*, *conc*, and *alpha*. *size* is calculated by summing ADC values of hit tubes. Cerenkov image is approximated with the ellipse, and its width and length are expressed as *width* and *length*. *alpha* is the angle between the major axis of the Cerenkov image and the line connecting the centroid of the image and the target star. The gamma rays from the target star showed a small angle in *alpha*; however, the cosmic rays were distributed from 0° to 90° uniformly. *conc* represents the concentration of photon intensities in the image. The detail can be seen in Hillas (1985). The events with images located near the camera boundary were cut by requiring the condition $R = (x^2 + y^2)^{1/2} \leq 1°8$, because the images near the camera boundary were distorted. The gamma rays showed the compact images compared with the hadronic showers, so we then selected the events that had a smaller *width* and *length* region, similar to what is predicted by a Monte Carlo simulation. We selected events with the following conditions: $width \leq W_{30} + 0.020 \ln (size/400)$, and $length \leq L_{50} + 0.023 \ln (size/400)$, where W_{30} and L_{50} correspond to 30% and 50% of the points obtained by integrating the width

Mkn501
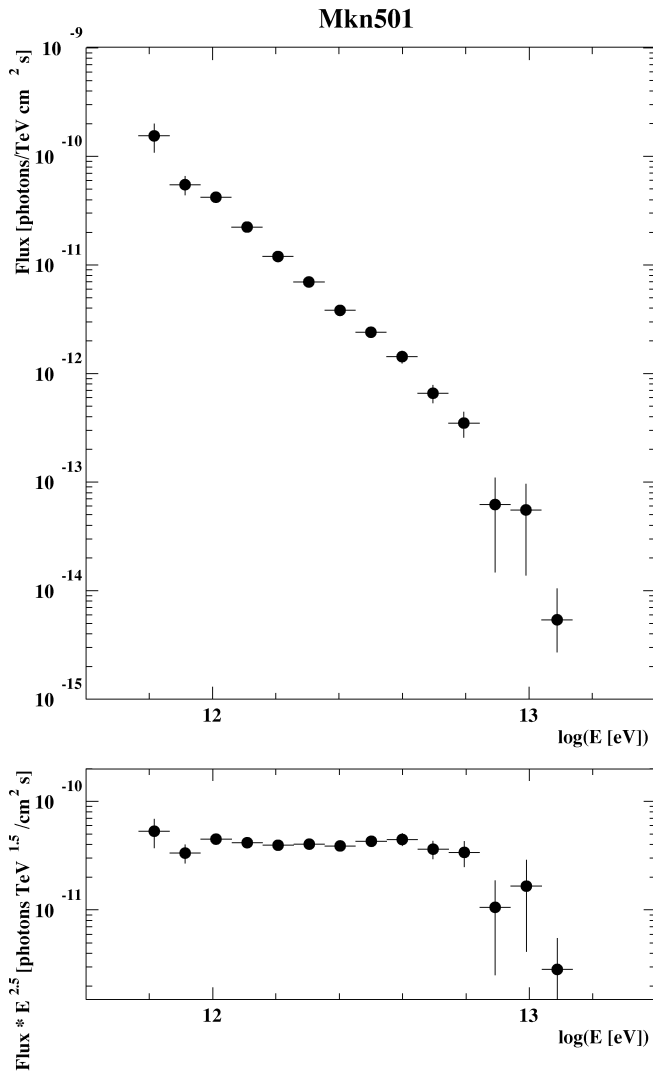
FIG. 2.—(*Top*) Differential energy spectrum of gamma rays from Mrk 501. (*Bottom*) Same, multiplied by $E^{2.5}$ to show the detail structure of the spectrum.

distribution from off-source events (Hadron events). The typical values of W_{30} and L_{50} are $0°.15$ and $0°.35$, respectively, and they naturally contain the zenith angle dependencies and the weather conditions. We could then obtain the constant fraction of data as gamma-ray candidates. The *size* of 400 corresponds to the average value of *size*. The second terms (0.020 and 0.023) represent the *size* dependence of the images as predicted by the Monte Carlo simulation. The parameter $conc \geq C_{50}$ corresponds to the light concentration, since gamma-ray showers have a higher light concentration than hadronic showers. After these selections, 8%–10% of the events remained. Finally, we selected for gamma-ray showers using the directional information obtained by the asymmetry of shower images. We selected for events that develop from neighboring the target source to the outer direction. Finally, 97% of the hadronic showers were rejected, and 30%–40% of gamma rays are selected. After these cuts, we obtained the excess of 35 σ from the direction of Mrk 501. The monthly excesses in the alpha distribution are shown in Figure 1.

3.1. *Energy Spectrum*

The absolute gain calibration was carried out by the measurement of a single photoelectron. We found that a single photoelectron corresponds to four ADC counts. The relative gain of each of the 256 channels is adjusted to within 5% accuracy using the LED pulser. We confirmed that the *size* distribution observed is consistent with the simulated showers assuming the cosmic-ray energy spectra in each composition. The uncertainty of the absolute gain or the *size*, and the energy relation was estimated as to be 20%. With a Monte Carlo simulation, we can determine the effective area for gamma rays and hadrons, $S_g(size)$ and $S_h(size)$. We also obtained experimentally the number of the excess events $N_{ex}(size)$ and the number of background events $N_{bg}(size)$. In order to minimize the systematic errors, we took the ratio $R(size) = [N_{ex}(size)/N_{bg}(size)]/[S_g(size)/S_h(size)]$. The denominator S_g/S_h has a weak dependence on *size* with our imaging selection of approximately $size^{0.4-0.5}$. The energy and the *size* relations for gamma rays and hadrons were determined by our Monte Carlo simulation to be $E_g = size/300$ TeV and $E_h = size/100$ TeV, respectively. Then we could obtain the gamma-ray energy spectrum from $dF/dE \propto R(size)(dF/dE_h)$. The derived energy spectrum is shown in Figure 2; $dF/dE = (4.0 \pm 0.2) \times 10^{-11}(E/1\ \text{TeV})^{-2.5 \pm 0.1}/\text{TeV cm}^2$ s. The differential energy spectrum can be well fitted with the power-law spectrum of index
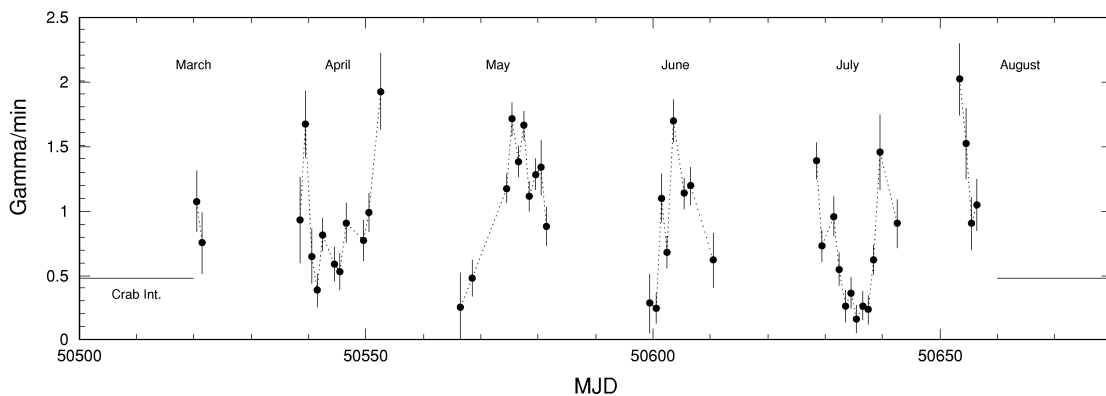
FIG. 3.—Time variation of the intensity of gamma rays from Mrk 501. For reference, the gamma-ray rate from the Crab Nebula measured by our detectors is shown by a horizontal line.
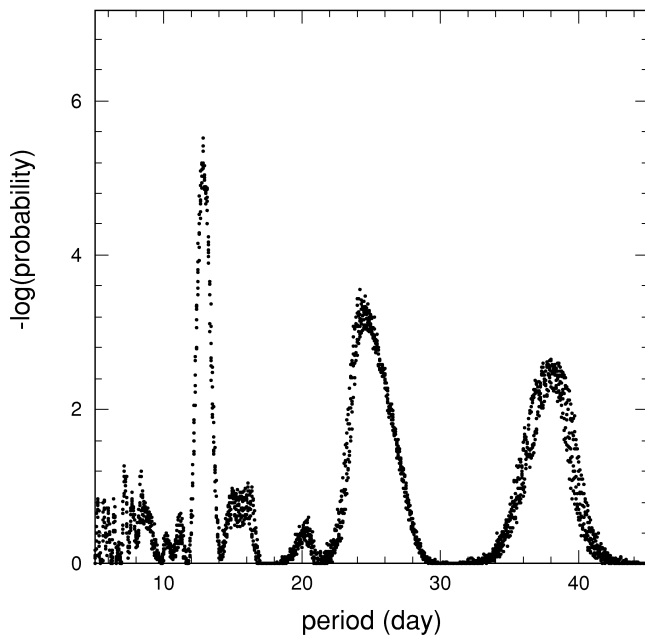
Fig. 4.—Periodicity test; Rayleigh tests are carried out assuming the test period. The amplitude is calculated in each test period, and the occurrence of the amplitude is evaluated using 10^7 false data sets, which also have time gaps between observing sessions. After taking account of independent trials for test period, the chance probability can be evaluated as $\sim 10^{-4}$.

-2.5. The spectrum became steeper above 5 TeV, which suggests a cutoff of the energy spectrum. However, it is possible that statistical fluctuations may be responsible for this effect. We need more statistics to obtain conclusive results. The saturation of the photomultipliers, the amplifiers, and the ADC is thought to occur at higher energy, above 30 TeV. We could minimize this saturation effect by the above ratio method.

3.2. Time Variation

Observation of the Mrk 501 was carried out for 47 nights from the end of March to the end of July. The gamma-ray event rate is plotted as a function of MJD in Figure 3. For reference, the gamma-ray rate from the Crab Nebula measured by our detectors is shown by a horizontal line. The event rate was highly variable day by day; the maximum event rate was about 4 crab, and the minimum rate was 0.3 ± 0.3 crab. The time-

scale of the intensity change was about a few days. We searched for a short time variation of the intensity, but we could not find clear evidence of any short time variation in our data set.

We can see high states and low states clearly in our data set. This feature (the timescale and the intensity change) in April and in July appeared to be similar, showing U shapes, and the interval of the two high states are 14 days and 12 days. May and June data each showed only one high state Λ shape. This is suggestive of a possible periodicity at 12–14 days, or 24–26 days. Using the Rayleigh statistics we found a possible 12.7 day periodicity as shown in Figure 4, and attempting to take into account aliasing with the period between observing sessions, we estimated the chance probability to be $\sim 10^{-4}$. However, we cannot completely rule out the possibility of the peak at 12.7 days being an artifact owing to the gaps in the observations. We need more observations to obtain the clear result about the periodicity of TeV gamma-ray intensity.

4. DISCUSSION

We obtained the differential energy spectrum of the gamma rays from Mrk 501. It shows a possible cutoff feature above 5–7 TeV. This cutoff is predicted to be caused by the interaction with the infrared photons or the limit of the electron acceleration in the jet. The cutoff energy of the gamma rays caused by the infrared photon interaction from the distance of the Mrk 501, $z = 0.034$, was estimated to be 7–15 TeV by Stecker & de Jager (1997).

In the time variation of the gamma-ray intensities, we found a possible periodicity, which may be a quasi-periodic oscillation. The observed data suggested the periodicity at 12–14 days, or 24–26 days. The relationship of this periodicity with high-energy phenomena around massive black holes could be influenced by factors including the precession of the jet, and the rotation of the black hole(s). R. Protheroe et al. (1997) suggested the interaction of the shock wave and the helical structure of the jet may cause this observed type of periodicity.

REFERENCES

Aiso, S., et al. 1997a, Proc. 25th Int. Cosmic-Ray Conf. (Durban), 3, 261
———. 1997b, Proc. 25th Int. Cosmic-Ray Conf. (Durban), 3, 177
———. 1997c, Proc. 25th Int. Cosmic-Ray Conf. (Durban), 5, 373
Barrau, A., et al. 1997, preprint (astro-ph/9710259)
Bradbury, S. M., et al. 1997, A&A, 320, L5
Catanese, M., et al. 1997a, preprint (astro-ph/9712325)
———. 1997b, ApJ, 487, L143

Hillas, A. M. 1985, Proc. 19th Int. Cosmic-Ray Conf. (La Jolla), 3, 445
Petry, D., et al. 1996, A&A, 311, L13
Protheroe, R. J., et al. 1997, preprint (astro-ph/9710118)
Punch, M., et al. 1992, Nature, 358, 477
Quinn, J., et al. 1996, ApJ, 456, L83
Shrader, C. R., & Gehrels, N. 1995, PASP, 107, 1
Stecker, F. W., & DeJager, O. C. 1997, preprint (astro-ph/9710145)